Structural Engineering and Mechanics, *Vol. 56, No. 4 (2015) 589-603*
DOI: http://dx.doi.org/10.12989/sem.2015.56.4.589

Computation of 2-D mixed-mode stress intensity factors by Petrov-Galerkin natural element method

Jin-Rae Cho*

Department of Naval Architecture and Ocean Engineering, Hongik University, Sejong 339-701, Korea

(Received October 13, 2014, Revised November 2, 2015, Accepted November 3, 2015)

Abstract. The mixed-mode stress intensity factors of 2-D angled cracks are evaluated by Petrov-Galerkin natural element (PG-NE) method in which Voronoi polygon-based Laplace interpolation functions and CS-FE basis functions are used for the trial and test functions respectively. The interaction integral is implemented in a frame of PG-NE method in which the weighting function defined over a crack-tip integral domain is interpolated by Laplace interpolation functions. Two Cartesian coordinate systems are employed and the displacement, strains and stresses which are solved in the grid-oriented coordinate system are transformed to the other coordinate system aligned to the angled crack. The present method is validated through the numerical experiments with the angled edge and center cracks, and the numerical accuracy is examined with respect to the grid density, crack length and angle. Also, the stress intensity factors obtained by the present method are compared with other numerical methods and the exact solution. It is observed from the numerical results that the present method successfully and accurately evaluates the mixed-mode stress intensity factors of 2-D angled cracks for various crack lengths and crack angles.

Keywords: 2-D angled crack; mixed-mode stress intensity factor (SIF); interaction integral; Petrov-Galerkin natural element (PG-NE) method; crack length and angle

1. Introduction

The calculation of stress intensity factors at the crack tip has been a great challenging subject in fracture mechanics during several decades. The cracked bodies are characterized by a non-convex domain, where both the stress and strain fields exhibit the $1/\sqrt{r}$ singularity at the crack tip. This kind of geometry-induced singularity is not confined to the cracked bodies, but it occurs at all the science and engineering problems defined over the convex domain characterized by the cornering angle greater than 180°. The stress singularity which is restricted within the extremely small region near the crack tip can not be successfully captured by the standard finite element method without employing specially-devised finite element or numerical technique. It is because there is a limitation in increasing the total number of finite elements to sufficiently interpolate the extremely high gradient of displacement field in the radial direction towards the crack tip. This numerical difficulty in calculating the stress intensity factors could be overcome by employing either the *J*-integral method, an alternative indirect method, or the specially-devised singular elements. The *J*-

*Corresponding author, Associate Professor, E-mail: jrcho@hongik.ac.kr

http://www.techno-press.org/?journal=sem&subpage=8 ISSN: 1225-4568 (Print), 1598-6217 (Online)

integral was introduced by Cherepanov (1967), Rice (1968) to accurately calculate the strain energy release rate with which the near-tip stress field would be asymptotically expressed in terms of the stress intensity factor (*SIF*). Meanwhile, since the 1970s, several investigators (Rice and Tracy 1973, Henshell and Shaw 1975, Barsoum 1976, Hibbitt 1977) introduced the singular elements which can represent the $1/\sqrt{r}$ singularity in stress field. More recently, Xiao *et al*. (2004) extended the hybrid crack element originated by Tong *et al*. (1973) in order for the direct evaluation of stress intensity factors and the coefficients of the higher order terms of the crack tip asymptotic field. Liu *et al*. (2004) improved the extended finite element method (XFEM) to directly evaluate mixed-mode stress intensity factors without extra post-processing.

The numerical calculation of stress intensity factors were traditionally made by either the *J*-integral method or the interaction integral method. Since the late 1990s, the extension of meshfree method to this problem have been actively progressed, in particular for the calculation of stress intensity factors by the interaction integral method, inspired by the fact that the interpolation functions used in meshfree methods provide the high smoothness. Belytschko *et al*. (1995) applied the element-free Galerkin (EFG) method to compute the singular stress fields and the stress intensity factors in 2-D fracture problems involving fatigue crack growth, dynamic crack propagation and interface cracks. Fleming *et al*. (1997) enriched the EFG method by adding asymptotic fields to the trial function and augmenting the basis function by the asymptotic fields, in order to accurately calculate stress intensity factors with fewer degrees of freedom. Rabczuk and Belytschko (2004) introduced a simplified meshfree method for arbitrary cracks by particle methods, in which the crack is treated as a collection of cracked particles and the cracking criterion is checked independently at each particle. Pant *et al*. (2011) introduced a new enrichment criterion for modeling the kinked cracks using the EFG method to compute SIF and simulate the quasi-static crack growth. Ching and Batra (2011) enriched the polynomial basis functions in the meshless local Petrov-Galerkin (MLPG) method with the crack tip singular fields to predict the singular stress fields near a crack tip and stress intensity factors. Rao and Rahman (2000) applied the EFG method to calculate the stress intensity factor and to simulate the crack propagation in 2-D linear fracture problems under mode-I and mixed-mode loading conditions. Fan *et al*. (2004), Shi *et al*. (2013) enriched the partition-of-unity (POU) method to calculate the stress intensity factors of 2-D angled cracks and to solve multiple crack problems. Singh *et al*. (2012) applied XFEM to evaluate the fatigue life of homogeneous plate containing multiple discontinuities such as holes, inclusions and minor cracks. Bhardwaj *et al*. (2015) combined XFEM and the extended isogeometric analysis (XIGA) to simulate the fatigue crack growth in functionally graded materials (FGMs) having multiple discontinuities.

Even though these methods provide the highly smooth interpolation functions, it is widely known that those suffer from the common difficulties in the enforcement of essential boundary condition and the numerical integration. Differing from these grid-point based meshfree methods, the natural element method (NEM) introduced originally by Braun and Sambridge (1995) uses the basis functions defined based on the Voronoi diagram and Delaunay triangulation. The basis functions called by Laplace interpolation function used in NEM not only exhibit the high smoothness (Sukumar and Moran 1999), but those satisfy the Kronecker delta property (Sambridge *et al*. 1995). Thanks to the Kronecker delta property and the introduction of Delaunay triangulation, the natural element method does not lead to difficulties in imposing the essential boundary condition and employing the traditional Gauss quadrature rule for the numerical integration (Sukumar *et al*. 1998, Cho and Lee 2006a), except that it may require a special technique such as the Sambridge's algorithm (Braun and Sambridge 1995) for non-convex

domain. This method has been refined and extended to solve the important engineering problems in linear and nonlinear solid mechanics by subsequent researchers (Yvonnet *et al*. 2004, Peña *et al*. 2008, Chenesta *et al*. 2011, Nie *et al*. 2011).

As an extension of our previous works (Cho and Lee 2006b, 2007, 2014), this paper intends to extend the Petrov-Galerkin natural element (PG-NE) method to the computation of mixed-mode stress intensity factors of 2-D angled cracks. To overcome the numerical integration inaccuracy caused by the discrepancy between the supports of test and basis functions, PG-NE method uses Voronoi polygon-based Laplace interpolation functions and CS-FE basis functions for the trial and test functions, respectively. The interaction integral is implemented in the frame of PG-NE method for which a crack-tip integration domain is defined by specifying the domain defining radius and the weighting function is interpolated in terms of Laplace interpolation functions. The appropriate value of domain defining radius is chosen through the preliminary parametric numerical experiment. And, two Cartesian coordinate systems are employed for the sake of mathematical derivation and easy numerical implementation, and the displacement, strains and stresses which are solved in the grid-oriented coordinate system are transformed to the other coordinate system aligned to the angled crack. The numerical experiments are carried out with the angled edge and center cracks to examine the validity and numerical accuracy of the present method. The stress intensity factors are evaluated for various grid densities, crack lengths and crack angles and compared with the other numerical methods and the exact solution.

2. Problem description

2.1 2-D linear elasticity with angled cracks

Let us consider a 2-D linear elastic body shown in Fig. 1 with cracks inclined by α which occupies an open bounded domain $\Omega \in \Re^2$ with the boundary $\partial\Omega = \Gamma_D \cup \underline{\Gamma_N \cup \Gamma_c}$. Here, Γ_D denotes the displacement boundary, Γ_N the traction boundary, and $\Gamma_c = \Gamma_c^+ \cup \Gamma_c^-$ the crack surface. For the sake of numerical implementation, we use two Cartesian coordinate systems, {*O*, *x*, *y*} for the 2-D linear elasticity problem and {*O*′, *x*′, *y*′} for the computation of stress intensity factor of angled crack respectively. Assuming the crack surface is traction-free, then the displacement field $\boldsymbol{u}(\boldsymbol{x})$ of the cracked body in the Cartesian coordinate system {*O*, *x*, *y*} is governed by the static equilibrium

$$\nabla \cdot \boldsymbol{\sigma} + \boldsymbol{b} = 0 \quad in \quad \Omega \tag{1}$$

with the displacement boundary condition

$$\boldsymbol{u} = \hat{\boldsymbol{u}} \quad on \quad \Gamma_D \tag{2}$$

and the traction boundary condition given by

$$\boldsymbol{\sigma} \cdot \boldsymbol{n} = \begin{cases} \hat{\boldsymbol{t}} & on \quad \Gamma_N \\ 0 & on \quad \Gamma_c^{\pm} \end{cases} \tag{3}$$

In which σ indicates the Cauchy stress, $\boldsymbol{b}$ the body force, $\boldsymbol{n}$ the outward unit vector normal to $\partial\Omega$ and $\hat{\boldsymbol{t}}$ the surface force. In addition, the Cauchy strain $\boldsymbol{\varepsilon}$ is defined by the (3×2) gradient-like operator $\boldsymbol{L}$ such that

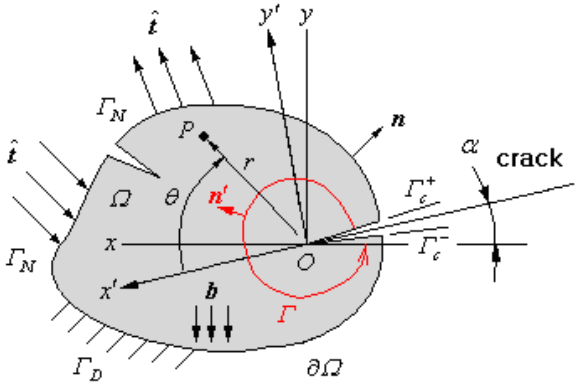

Fig. 1 A 2-D linear elastic body with angled edge cracks

$$\boldsymbol{\varepsilon} = \boldsymbol{\varepsilon}(\boldsymbol{u}) = \boldsymbol{L}\boldsymbol{u} \tag{4}$$

for small displacement and strains, and the stresses and strains are constituted by using the Hooke tensor $\boldsymbol{E}$ of Lame constants

$$\boldsymbol{\sigma} = \boldsymbol{E} : \boldsymbol{\varepsilon} \tag{5}$$

For two-dimensional planar configuration, the enery release rate per unit crack extension in the x'-direction can be defined by the path-independent J-integral given by

$$J = \int_{\Gamma} \left(W\delta_{1j} - \sigma_{ij} \frac{\partial u_i}{\partial x_1'} \right) n_j' ds \tag{6}$$

using the indicial notation (i.e., $x_1' = x'$ and $x_2' = y'$). Here, $\boldsymbol{W}=\boldsymbol{\sigma}\cdot\boldsymbol{\varepsilon}/2$ is the strain energy density and $\boldsymbol{n}'$ denotes the outward unit vector normal to an arbitrary path Γ enclosing the crack tip in a counter-clock wise sense. For a mixed-mode crack problem, the energy release rate J is related to the stress intensity factors such that

$$J = \frac{K_I^2 + K_{II}^2}{\overline{E}} \tag{7}$$

according to Irwin's relation (1957). Here, $\overline{E}$ becomes E for the plane stress state and $E/(1-\nu^2)$ for the plane strain state, respectively. Note that the displacement, strains and stresses are calculated based on the grid-oriented coordinate system $\{O, x, y\}$ and then transformed to the values in the crak-line oriented coordinate system $\{O, x', y'\}$ by the chain rule.

2.2 Interaction integral for mixed-mode stress intensity factors

Two stress intensity factors K_I and K_{II} in Eq. (7) can be extracted using the interaction integral which considers two equilibrium states of a cracked body. Here, state 1 is the actual equilibrium state of a body subject to the prescribed boundary conditions while state 2 denotes an auxiliary equilibrium state which corresponds to the asymptotic crack-tip displacement and stress fields. The interaction integral denoted by $M^{(1,2)}$ for the two equilibrium states is defined by

$$M^{(1,2)} = \int_{\Gamma} \left[W^{(1,2)} \delta_{1j} - \sigma_{ij}^{(1)} \frac{\partial u_i^{(2)}}{\partial x_1'} - \sigma_{ij}^{(2)} \frac{\partial u_i^{(1)}}{\partial x_1'} \right] n_j' ds \tag{8}$$

where $W^{(1,2)}$ denotes the mutual strain energy density defined by $W^{(1,2)}=[\boldsymbol{\sigma}^{(1)} \cdot \boldsymbol{\varepsilon}^{(2)} + \boldsymbol{\sigma}^{(2)} \cdot \boldsymbol{\varepsilon}^{(1)}]/2$. Meanwhile, the J-integral for the combined two equilibrium states is expressed by

$$\begin{aligned} J^{(1+2)} &= \int_{\Gamma} \left[\frac{1}{2} \left(\sigma_{ij}^{(1)} + \sigma_{ij}^{(2)} \right) \left(\varepsilon_{ij}^{(1)} + \varepsilon_{ij}^{(2)} \right) \delta_{1j} - \left(\sigma_{ij}^{(1)} + \sigma_{ij}^{(2)} \right) \frac{\partial \left(u_i^{(1)} + u_i^{(2)} \right)}{\partial x_1'} \right] n_j' ds \\ &= J^{(1)} + J^{(2)} + M^{(1,2)} \end{aligned} \tag{9}$$

with $J^{(1)}$ and $J^{(2)}$ being the energy release rates for states 1 and 2, respectively. For the combined case of states 1 and 2, Irwin's relation (7) implies that

$$\begin{aligned} J^{(1+2)} &= \frac{1}{\overline{E}} \left[\left(K_I^{(1)} + K_I^{(2)} \right)^2 + \left(K_{II}^{(1)} + K_{II}^{(2)} \right)^2 \right] \\ &= J^{(1)} + J^{(2)} + \frac{2}{\overline{E}} \left(K_I^{(1)} K_I^{(2)} + K_{II}^{(1)} K_{II}^{(2)} \right) \end{aligned} \tag{10}$$

Equating Eq. (9) and Eq. (10) leads to the following relation give by

$$M^{(1,2)} = \frac{2}{\overline{E}} \left(K_I^{(1)} K_I^{(2)} + K_{II}^{(1)} K_{II}^{(2)} \right) \tag{11}$$

The stress intensity factor $K_I^{(1)}$ for mode I can be determined by making state 2 be the pure mode I asymptotic field in which $K_I^{(2)} = 1$ and $K_{II}^{(2)} = 0$

$$M^{(1,\text{Mode I})} = \frac{2}{\overline{E}} K_I^{(1)} \tag{12}$$

In a similar manner, the stress intensity factor K_{II} of mode II can be also determined.

The line integral (8) is not always best for numerical calculation because the integration of displacement gradients, strains and stresses of states 1 and 2 along the non-regular arbitrary path Γ becomes rather painstaking. Thus, it is desired to be transformed into an area integral form, for which Eq. (8) is firstly rewritten as

$$M^{(1,2)} = \int_{C} \left[\sigma_{ij}^{(1)} \frac{\partial u_i^{(2)}}{\partial x_1'} + \sigma_{ij}^{(2)} \frac{\partial u_i^{(1)}}{\partial x_1'} - W^{(1,2)} \delta_{1j} \right] q m_j' ds \tag{13}$$

by extending the path Γ to $C = \Gamma + \Gamma_c^- + \Gamma_c^+ + \Gamma_o$ along two crack faces as shown in Fig. 2 and by multiplying a sufficiently smooth weighting function $q(\boldsymbol{x})$. It is not hard to realize that Eqs. (8) and (13) become identical when $q(\boldsymbol{x})$ becomes unity on Γ and vanishes on Γ_o, together with the fact that the crack faces are traction free and straight in the darkened donut-type region A.

By taking the divergence theorem to Eq. (13) and letting the inner path Γ be shrunk to the crack tip, the transformed line integral (13) ends up with

$$M^{(1,2)} = \int_{A} \left[\sigma_{ij}^{(1)} \frac{\partial u_i^{(2)}}{\partial x_1'} + \sigma_{ij}^{(2)} \frac{\partial u_i^{(1)}}{\partial x_1'} - W^{(1,2)} \delta_{1j} \right] \frac{\partial q}{\partial x_j'} dA \tag{14}$$

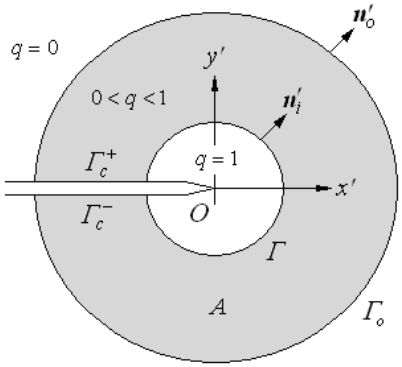

Fig. 2 An extended closed path Γ, the integral domain A and the weighting function $q(x)$

All the quantities in Eq. (14) are evaluated with respect to the crack-line oriented Catesian coordinate system $\{O, x', y'\}$.

3. Numerical Implementation of the Interaction Integral by PG-NE Method

3.1 Petrov-Galerkin natural element method

The boundary value problem (1) in the strong form is converted to the weak form according to the usual virtual work principle: Find $\boldsymbol{u}(\boldsymbol{x})$ such that

$$\int_{\Omega} \boldsymbol{\varepsilon}(\boldsymbol{v}) : \boldsymbol{\sigma}(\boldsymbol{u}) dv = \int_{\Omega} \boldsymbol{b} \cdot \boldsymbol{v}\, dv + \int_{\Gamma_N} \hat{\boldsymbol{t}} \cdot \boldsymbol{v}\, ds \tag{15}$$

for every admissible displacement field $\boldsymbol{v}(\boldsymbol{x})$ in the grid-oriented Cartesian coordinate system $\{O, x, y\}$. In order for the Petrov-Galerkin natural element approximation using a given non-convex natural element grid $\Im_{NEM}$ composed of N grid points and Delaunay triangles as shown in Fig. 3(a), trial and test displacement fields $\boldsymbol{u}(\boldsymbol{x})$ and $\boldsymbol{v}(\boldsymbol{x})$ are expanded as

$$\boldsymbol{u}_h(\boldsymbol{x}) = \sum_{J=1}^{N} \boldsymbol{u}_J \phi_J(\boldsymbol{x}) = \boldsymbol{\Phi}\, \bar{\boldsymbol{u}}\,, \qquad \boldsymbol{v}_h(\boldsymbol{x}) = \sum_{I=1}^{N} \boldsymbol{v}_I \psi_I(\boldsymbol{x}) = \boldsymbol{\Psi}\, \bar{\boldsymbol{v}} \tag{16}$$

with Laplace interpolation functions $\phi_J(\boldsymbol{x})$ shown in Fig. 3(b) and CS-FE basis functions $\psi_I(\boldsymbol{x})$. The reader may refer to the references (Cho and Lee 2006a, Cho *et al*. 2013) for more details on the CS-FE basis function defined on three-node trangular elements and the definition of Laplace interpolation fuctions. Meanwhile, Φ and Ψ denote $(2\times 2N)$ matrices containing N basis functions ϕ_J and ψ_I, and $\bar{\boldsymbol{u}}$ and $\bar{\boldsymbol{v}}$ are the $(2N\times 1)$ nodal vectors, respectively.

Substituting Eq. (16) into Eqs. (4)-(5) and (15) leads to the simultaneous linear equations in matrix form given by

$$[\boldsymbol{K}]\bar{\boldsymbol{u}} = \{\boldsymbol{F}\} \tag{17}$$

Here, the global stiffness matrix $[\boldsymbol{K}]$ and the global load vector $\{\boldsymbol{F}\}$ are constructed as following

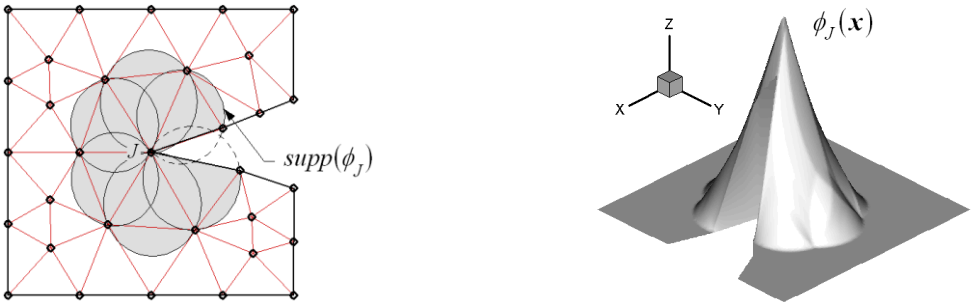

(a) (b)

Fig. 3 (a) Non-convex NEM grid $\Im_{NEM}$, (b) Laplace interpolation function $\phi_J(\boldsymbol{x})$

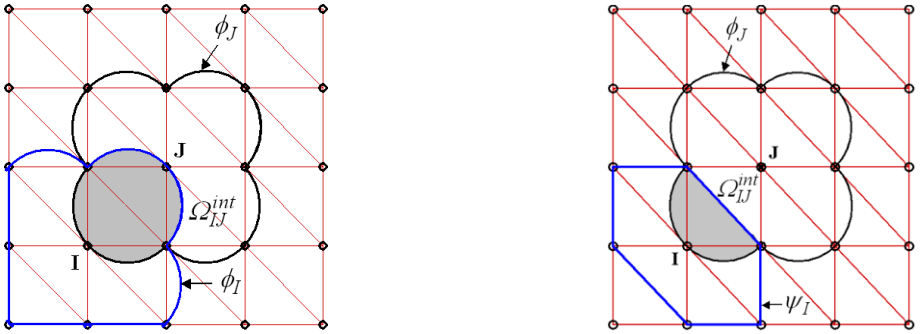

(a) (b)

Fig. 4 Intersection Ω_{IJ}^{int} between trial function and test function: (a) ϕ_I and ϕ_J in BG-NEM, (b) ψ_I and ϕ_J in PG-NEM

$$[\boldsymbol{K}]=\sum_{I=1}^{N}\boldsymbol{K}_I, \quad \{\boldsymbol{F}\}=\sum_{I=1}^{N}\boldsymbol{F}_I \tag{18}$$

with the node-wise stiffness matrices and load vectors defined by

$$\boldsymbol{K}_I=\int_{\Omega_v^I}(\boldsymbol{L}\Psi)^T\boldsymbol{E}(\boldsymbol{L}\Phi)dv \tag{19}$$

$$\boldsymbol{F}_I=\int_{\Omega_v^I}\Psi^T\boldsymbol{b}\,dv+\int_{\Gamma_N\cap\Omega_v^I}\Psi^T\hat{\boldsymbol{t}}\,ds \tag{20}$$

Here, $\Omega_v^I=supp(\psi_I(\boldsymbol{x}))$ indicates the support of I-th CS-FE basis function and $\boldsymbol{E}$ indicates the (3×3) material constant matrix of linear elasticity. It is noted that the numerical integration in the natural element method is carried out Delaunay triangle by Delaunay triangle.

According to Strang and Fix (1973), the numerical integration accuracy and the convergence rate of the Gauss quadrature rule deteriorates if the support of integrand function does not coincide with a regular integration region where the regular Gauss quadrature rule is applied. As shown in Fig. 5(a) for the Buvnov-Galerkin natural element (BG-NE) method in which Laplace interpolation functions $\phi_J(\boldsymbol{x})$ are used for both the test and trial functions, neither the support of trial basis function ϕ_I nor the intersection Ω_{int}^{IJ} (i.e., a darkened circle) between ψ_I and ϕ_J does not

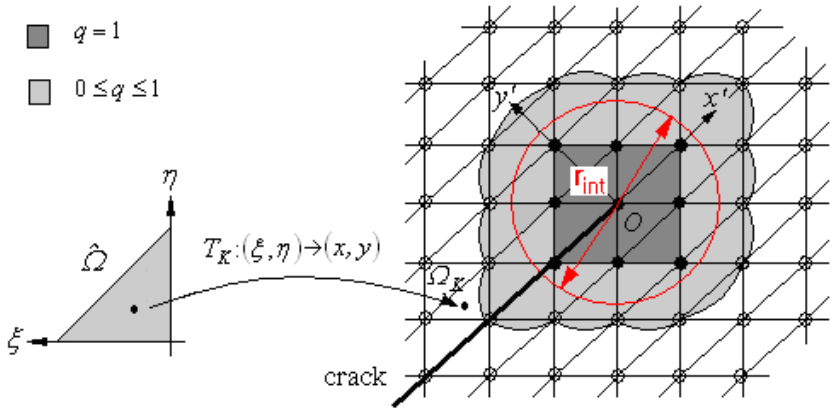

Fig. 5 The construction of the integral domain A and the weighting function $q(x)$

coincide with a union of Delaunay triangles. For this reason, one encounters the numerical difficulty in calculating $\boldsymbol{K}_I$ and $\boldsymbol{F}_I$ in Eqs. (19) and (20). In order to avoid such a numerical integration difficulty, the PG-NE method uses the constant strain finite element (CS-FE) basis function as the test basis function. As shown in Fig. 4(b), its support is composed of a union of Delaunay triangles, so that the discrepancy between the regular Gauss integration domain and the test function support does not occur any more. Furthermore, the intersection region Ω_{int}^{IJ} between the CS-FE basis function ψ_I and Laplace basis function ϕ_J is always contained within $supp(\psi_I)$. Thus, one can accurately and easily integrate $\boldsymbol{K}_I$ and $\boldsymbol{F}_I$ by applying the Gauss quadrature rule, as for the finite element method.

3.2 Interaction integral by PG-NE method

The weighting function $q(\boldsymbol{x})$ specified in Fig. 2 should be sufficiently smooth such that its differentiation in the interaction integral (14) is integrable. In the current study, Laplace interpolation function $\phi_J(\boldsymbol{x})$ depicted in Fig. 3(b) which is also used for the trial function is used. Meanwhile, the crack-tip integral domain A is chosen by specifying its radius r_{int} as represented in Fig. 5. The value of unity is assigned to all the nodes within the circle, while the value of zero is specified to the remaining nodes within a whole NEM grid. Then, from the linearity property of Laplace interpolation function (Cho *et al*., 2013), a darkened rectangular region has the value of unity and its boundary serves as an interior path Γ shown in the previous Fig. 3. Meanwhile, another union of grayed Delaunay triangles have the value $0 \le q \le 1$ and its boundary becomes the outer path Γ_o. In other words, the union of grayed Delaunay triangles automatically becomes the integral domain A.

Let us denote M_A be the total number of grayed Delaunay triangles within the integral domain A, then the interaction integral (14) is integrated triangle by triangle such that

$$M^{(1,2)} = \sum_{K=1}^{M_A} M_K^{(1,2)} \tag{21}$$

with $M_K^{(1,2)}$ being the triangle-wise interaction integrals. It is because the gradient of weighting

function $\partial q/\partial x'_j$ vanishes outside the integral domain A. Here, each triangle-wise interaction integral is computed by

$$\begin{aligned} M_K^{(1,2)} &= \int_{\Omega_K} \left[\sigma_{ij}^{(1)} \frac{\partial u_i^{(2)}}{\partial x'_1} + \sigma_{ij}^{(2)} \frac{\partial u_i^{(1)}}{\partial x'_1} - W^{(1,2)} \delta_{1j} \right] \frac{\partial q}{\partial x'_j} dA \\ &= \sum_{\ell=1}^{INT} \left[\sigma_{ij}^{(1)} \frac{\partial u_i^{(2)}}{\partial x'_1} + \sigma_{ij}^{(2)} \frac{\partial u_i^{(1)}}{\partial x'_1} - W^{(1,2)} \delta_{1j} \right]_{\boldsymbol{x}_\ell} \left. \frac{\partial q}{\partial x'_j} \right|_{\boldsymbol{x}_\ell} w_\ell \left| \boldsymbol{J} \right|_{\boldsymbol{x}_\ell} \end{aligned} \tag{22}$$

using the chain rule and Gauss quadrature rule, in which INT, $\boldsymbol{x}_\ell$ and w_ℓ indicate the total number of integration points, sampling points and weights, respectively. Note that the sampling points $\boldsymbol{x}_\ell$ in Ω_K and the Jacobian $\left|\boldsymbol{J}\right|_{\boldsymbol{x}_\ell}$ are calculated using the geometry transformation T_K defined by

$$T_K : x_\ell = \sum_{i=1}^{3} x_i \psi_i(\xi,\eta)_\ell, \quad y_\ell = \sum_{i=1}^{3} y_i \psi_i(\xi,\eta)_\ell \tag{23}$$

between Ω_K in NEM grid and the master triangle element $\hat{\Omega}$. Here, $\{x_i, y_i\}$ are the co-ordinates of three nodes in each Delaunay triangle, $(\xi, \eta)_\ell$ the Gauss points in $\hat{\Omega}$, and ψ_i the triangular shape functions. Meanwhile, in two-dimensional fracture mechanics problems, the displacement and stress fields near the crack tip which are used for state 2 are referred to a book by Anderson (1991).

4. Numerical experiments

We first consider an angled edge crack shown in Fig. 6(a) subject to a uniform tensile distributed load, where L and H are equally set by 10 mm and the crack angle α is 45°. The load σ is set by 1000 Pa and Young's modulus and Poisson's ratio are 2.0×10^5 MPa and 0.25 respectively. The plate is assumed to be in plane stress condition and the relative crack length a/L is taken variable for the parametric investigation of *SIF*s. This problem was solved by several investigators, for example, Rooke and Cartwright (1976) using the boundary collocation method (BCM) and Zhang *et al*. (2008) by the enriched element-free Galerkin (EFG) method. Fig. 6(b) represents an integral domain A for the interaction integral in a uniform NEM grid by setting the domain defining radius r_{int} be two times of the square root of the area of a rectangular element composed of two Delaunay triangles. Referring to Fig. 5 illustrating the construction procedure of integral domain, the weighting function $q(\boldsymbol{x})$ has the value of $0 \le q \le 1$ within the grey region and unity in the central white region while it automatically vanishes over the remaining NEM region outside the grey region. The influence of the integral domain size on the calculation accuracy of stress intensity factors may refer to the papers by Moës *et al*. (1999), Rao and Rahman (2000). In the current study, the appropriate values of r_{int} for K_I and K_{II} are chosen by the preliminary parametric numerical experiments, and both the NEM structural analysis of cracked plates and the interaction integral for computing the stress intensity factors are commonly carried out using 13 Gaussian points. The reader may refer to our previous papers (Cho and Lee 2006a, 2014) for the verification of PG-NE method at the level of stress and strain. It has been justified that the stress distributions computed by this method is more accurate and stable than BG-NE method as well as conventional finite element method.

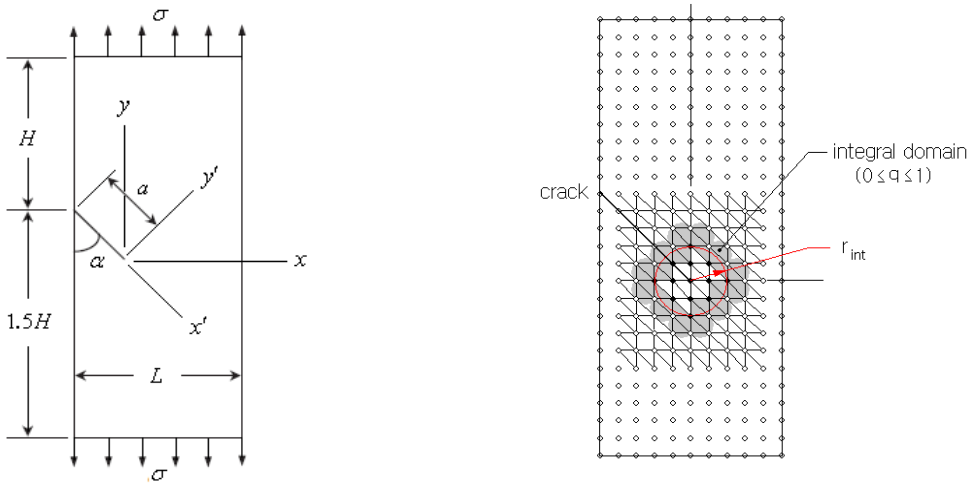

(a) (b)

Fig. 6 (a) A plate with an angled edge crack under a uniform tensile distributed load, (b) NEM grid and the integral domain

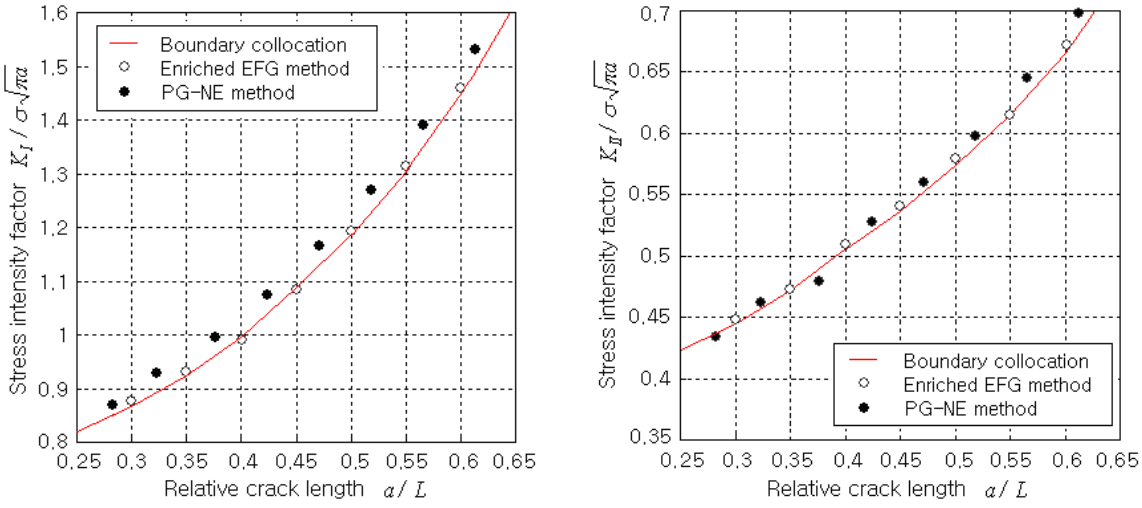

(a) (b)

Fig. 7 The normalized stress intensity factors of the angled edge crack: (a) $K_I / \sigma\sqrt{\pi a}$, (b) $K_{II} / \sigma\sqrt{\pi a}$

Fig. 7 compares the normalized stress intensity factors obtained by the present method with those obtained by the boundary collocation method (BCM) and the enriched EFG method (Zhang *et al*. 2008), for different relative crack lengths. A 30×75 uniform NEM grid is used for the present PG-NE method, and the domain defining radius r_{int} is set by 1.5 mm for K_I and 4.0 mm for K_{II}, respectively. It is observed that PG-NE method predicts the stress intensity factors slightly higher than two other methods, but the maximum relative differences with respect to the boundary collocation method are found to be 3.626% in K_I and 2.348% in K_{II} as given in Table 1. Thus, it has been confirmed that the present method accurately evaluates stress intensity factors of 2-D

Table 1 The computed stress intensity factors to the relative crack length

Relative crack length *a/L*	Normalized stress intensity factors			
	$K_I / \sigma\sqrt{a\pi}$		$K_{II} / \sigma\sqrt{a\pi}$	
	PG-NEM	BCM	PG-NEM	BCM
0.283	0.8702	0.8504	0.4342	0.4359
0.323	0.9287	0.8962	0.4623	0.4572
0.377	0.9961	0.9649	0.4790	0.4899
0.424	1.0742	1.0418	0.5281	0.5203
0.471	1.1645	1.1302	0.5596	0.5517
0.519	1.2688	1.2305	0.5980	0.5884
0.566	1.3896	1.3518	0.6450	0.6302
0.613	1.5297	1.4901	0.6975	0.6784

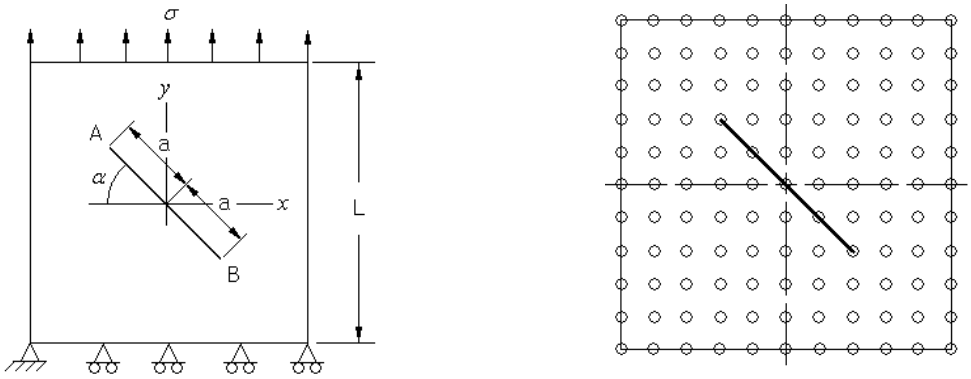

(a) (b)

Fig. 8 (a) A square plate with an angled center crack under a uniform tensile distributed load, (b) uniform NEM grid

angled crack without employing special numerical approximation or extra enrichment. It is noted that the *SIF*s of BCM in Table 1 at the specific relative crack lengths which are divided for PG-NE method are calculated by linearly interpolating those of BCM at the regular relative crack lengths (i.e., 0.3, 0.35, 0.4 and so on) on the plot.

Fig. 8(a) shows a square plate of L=20 *in* with an angled center crack which is in plane stress condition and subjected to a far-field uniform vertical distributed load σ equal to unity. The material properties are as follows: E=3.0×10^7 *psi* and v=0.25, and the crack of length 2a is oriented with an angle α with respect to the negative x-axis. Unform NEM grid shown in Fig. 8(b) is used and the total number of grid points is taken variable for the parametric experiment. According to Yau *et al*. (1980), Dolbow and Gosz (2002), the stress intensity factors which are analytically expressed in terms of the angle α are given by

$$K_I = \sigma\sqrt{\pi a}\cos^2\alpha, \qquad K_{II} = \sigma\sqrt{\pi a}\sin\alpha\cos\alpha \tag{24}$$

with a being the half crack length. For the convergence experiment with respect to the density of uniform NEM grid, the crack angle α is set by 45° and the grid density-dependent half crack length

Table 2 Variation of stress intensity factors to the grid density

NEM grid	Half crack length a (*in*)	Total number of nodes	K_I / K_I^{anal}		K_{II} / K_{II}^{anal}	
			tip A	tip B	tip A	tip B
50×50	3.394	2601	1.0147	0.9909	0.9940	1.0053
40×40	3.536	1681	1.0180	1.0035	0.9907	0.9810
30×30	3.771	961	1.0105	0.9529	1.0268	0.9792
20×20	4.243	441	0.9781	1.0602	1.0553	0.9051
10×10	5.657	121	0.8964	0.8599	0.8435	0.8656

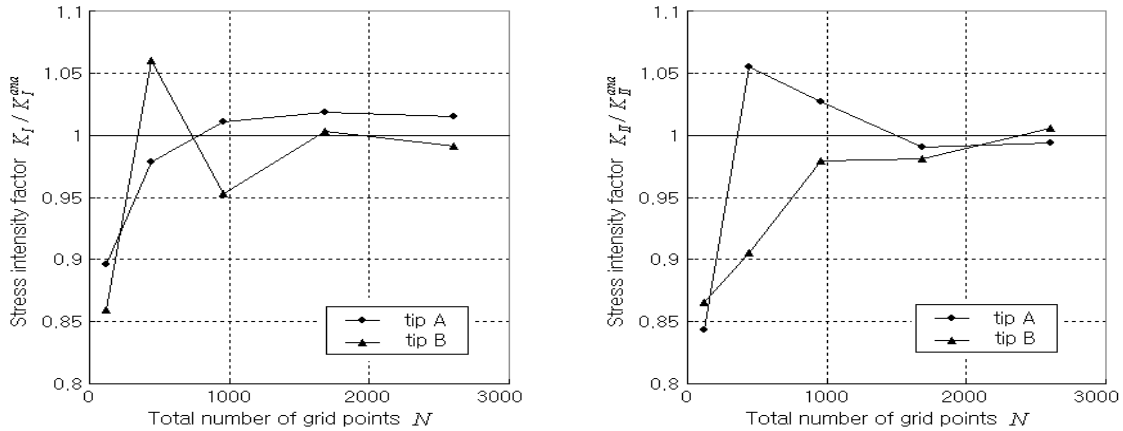

(a) (b)

Fig. 9 The convergence of stress intensity factors to the total number of nodes: (a) K_I / K_I^{ana}, (b) K_{II} / K_{II}^{ana}

a varies from 3.394 *in* to 5.657 *in* as given in Table 2.

Referring to Table 2, five uniform NEM grids are used and the ratios K_I / K_I^{anal} and K_{II} / K_{II}^{anal} of stress intensity factor are calculated at two crack tips A and B. As in the previous example, 13 Gauss points are used for both the NEM structural analysis and the interaction integral. It is clearly observed from Table 2 and Fig. 9 that the ratios of stress intensity factor approach unity as the grid density increases such that the NEM grids higher than 30×30 provide the stress intensity factors with the maximum relative error less than 2.0%. Thus, it has been verified that PG-NE method accurately predicts the stress intensity factors of angled crack with the practically reasonable grid density. Furthermore, it is clearly observed that the present method shows a uniform convergence to the grid density.

Fig. 10(a) represents the variation of stress intensity factors to the half crack length when the crack angle is 45°, where the exact values are calculated using Eq. (24). A 40×40 uniform NEM grid is used based on the previous convergence experiment and the stress intensity factors are calculated at crack tip B. It is observed that the stress intensity factors K_I and K_{II} are in good agreement with the exact values for the relative crack lengths of $0.071 \le a/L \le 0.354$. The maximum relative error equal to 5.66% with respect to the exact solution is occurred at a/L=0.247. Thus, it has been justified that the present method provides accurate stress intensity factors of center angled crack for various crack lengths. Fig. 10(b) represents the comparison of *SIF* ratios between

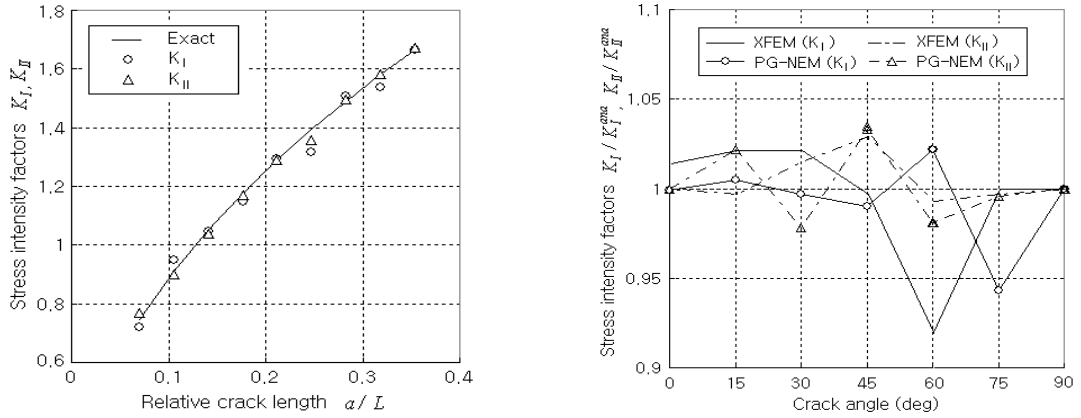

(a) (b)

Fig. 10 (a) Stress intensity factors to the half crack length, (b) ratios of stress intensity factor to the crack angle

the present method and XFEM by Liu *et al*. (2004). In the XFEM, a standard FE mesh is firstly generated without considering the existence of cracks, and then the standard continuous FE displacement is to be enriched with additional functions to model cracks. The discontinuous displacement fields and the leading terms of the asymptotic crack tip displacement fields are incorporated into the FE displacement field using the partition of unit method (Babuska and Melenk 1997). Since there is difficulty in keeping exactly the relative crack length of 0.05 for different crack angles, the *SIF* ratios are taken for the comparison between two methods. It is observed that the present method provides the numerical accuracy similar to XFEM.

5. Conclusions

The computation of 2-D mixed-mode stress intensity factors of angled cracks by Petrov-Galerkin natural element has been addressed in this paper, in which Laplace interpolation functions and CS-FE basis functions are used for the trial and test functions respectively to overcome the numerical integration inaccuracy. The interaction integral was formulated in the frame PG-NE method in which the donut-type integral domain and the weighting function were easily defined in terms of the domain defining radius and Laplace interpolation functions. In order to avoid the difficulties in mathematical formulation and numerical implementation, two Cartesian coordinate systems were used, a NEM grid-based one for the structural analysis and a crack tip-oriented one for the interaction integral, and the displacement and stress fields were transformed into the crack tip-oriented Cartesian coordinate system.

The characteristics of the present PG-NE method, in aspect of the calculation accuracy, were investigated through the numerical experiments of angled edge and center cracks. Through the experiment with the angled edge crack to the crack length, 2-D mixed-mode stress intensity factors were calculated for various crack lengths and it has been observed that PG-NE method predicts the stress intensity factors slightly higher than the boundary collocation method and the enriched element-free Galerkin method. But, it has been confirmed that the present method accurately predicts the mixed-mode stress intensity factors for a wide range of crack lengths without extra

enrichment such that the maximum relative differences with respect to two reference methods are 3.626% in K_I and 2.348% in K_{II} respectively. Meanwhile, through the experiment with the angled center crack to the grid density, it has been confirmed that the *SIF* ratios approach unity as the grid density increases such that the maximum relative error with respect to the exact solution is less than 20% when NEM grid is finer than 30×30. Furthermore, it has been observed that the stress intensity factors K_I and K_{II} at both crack tips are in good agreement with the exact values for the relative crack lengths of $0.071 \le a/L \le 0.354$. In addition, it has been verified that the numerical accuracy similar to XFEM for a wide range of crack angles.

References

Anderson, T.L. (1991), *Fracture Mechanics: Fundamentals and Applications*, 1st Edition, CRC Press.

Babuska, I. and Melenk, J.M. (1997), "The partition of unity method", *Int. J. Numer. Meth. Eng.*, **40**, 727-758.

Barsoum, R.S. (1976), "On the use of isoparametric finite elements in linear fracture mechanics", *Int. J. Numer. Meth. Eng.*, **10**, 25-38.

Belytschko, T., Lu, Y.Y., Gu, L. and Tabbara, M. (1995), "Element-free Galerkin methods for static and dynamic fracture", *Int. J. Solid. Struct.*, **32**(17-18), 2547-2570.

Bhardwaj, G., Singh, I.V. and Mishra, B.K. (2015), "Stochastic fatigue crack growth simulation of interfacical crack in bi-layered FGMs using XIGA", *Comput. Meth. Appl. Mech. Eng.*, **284**, 186-229.

Braun, J. and Sambridge, M. (1995), "A numerical method for solving partial differential equations on highly irregular evolving grids", *Nature*, **376**, 655-660.

Cherepanov, G.P. (1967), "The propagation of cracks in a continuous medium", *J. Appl. Math. Mech.*, **31**(3), 503-512.

Chinesta, F., Cescotto, S., Cueto, E. and Lorong, P. (2011), *Natural Element Method for the Simulation of Structures and Processes*, John Wiley & Sons, New Jersey.

Ching, H.K. and Batra, R.C. (2001), "Determination of crack tip fields in linear elastostatics by the meshless local Petrov-Galerkin (MLPG) method", *Comput. Model. Eng. Sci.*, **2**(2), 273-289.

Cho, J.R. and Lee, H.W. (2006a), "A Petrov-Galerkin natural element method securing the numerical integration accuracy", *J. Mech. Sci. Tech.*, **20**(1), 94-109.

Cho, J.R. and Lee, H.W. (2006b), "2-D large deformation analysis of nearly incompressible body by natural element method", *Comput. Struct.*, **84**, 293-304.

Cho, J.R. and Lee, H.W. (2007), "2-D frictionless dynamic contact analysis of large deformable bodies by Petrov-Galerkin natural element method", *Comput. Struct.*, **85**, 1230-1242.

Cho, J.R., Lee, H.W. and Yoo, W.S. (2013), "Natural element approximation of Reissner-Mindlin plate for locking-free numerical analysis of plate-like thin elastic structures", *Comput. Meth. Appl. Mech. Eng.*, **256**, 17-28.

Cho, J.R. and Lee, H.W. (2014), "Calculation of stress intensity factors in 2-D linear fracture mechanics by Petrov-Galerkin natural element method", *Int. J. Numer. Meth. Eng.*, **98**, 819-839.

Dolbow, J. and Gosz, M. (2002), "On the computation of mixed-mode stress intensity factors in functionally graded materials", *Int. J. Solid. Struct.*, **39**(9), 2557-2574.

Fan, S.C., Liu, X. and Lee, C.K. (2004), "Enriched partition-of-unity finite element method for stress intensity factors at crack tips", *Comput. Struct.*, **82**, 445-461.

Fleming, M., Chu, Y.A., Moran, B. and Belytschko, T. (1997), "Enriched element-free Galerkin methods for crack tip fields", *Int. J. Numer. Meth. Eng.*, **40**, 1483-1504.

Henshell, R.D. and Shaw, K.G. (1975), "Crack tip elements are unnecessary", *Int. J. Numer. Meth. Eng.*, **9**, 495-507.

Hibbitt, H.D. (1977), "Some properties of singular isoparametric elements", *Int. J. Numer. Meth. Eng.*, **11**, 180-184.

Irwin, G.R. (1957), "Analysis of stresses and strains near the end of a crack traveling a plate", *J. Appl. Mech.*, **24**, 361-364.

Liu, X.Y., Xiao, Q.Z. and Karihaloo, B.L. (2004), "XFEM for direct evaluation of mixed mode SIFs in homogeneous and bi-materials", *Int. J. Numer. Meth. Eng.*, **59**, 1103-1118.

Moës, N., Dolbow, J. and Belytschko, T. (1999), "A finite element method for crack growth without remeshing", *Int. J. Numer. Meth. Eng.*, **46**, 131-150.

Nie, Z.F., Zhou, S.J., Han, R.J., Xiao, L.J. and Wang, K. (2011), "C^1 natural element method for strain gradient linear elasticity and its application to microstructures", *Acta Mechanica Sinica*, **28**(1), 91-103.

Pant, M., Singh, I.V. and Mishra, B.K. (2011), "A novel enrichment criterion for modeling kinked cracks using element free Galerkin method", *Int. J. Mech. Sci.*, **68**, 140-149.

Peña, E., Martinez, M.A., Calvo, B. and Doblaré, M. (2008), "Application of the natural element method to finite deformation inelastic problems in isotropic and fiber-reinforced biological soft tissues", *Comput. Meth. Appl. Mech. Eng.*, **197**(21-24), 1983-1996.

Rabczuk, T. and Belytschko, T. (2004), "Cracking particles: a simplified meshfree method for arbitrary evolving cracks", *Int. J. Numer. Meth. Eng.*, **61**, 2316-2343.

Rao, B.N. and Rahman, S. (2000), "An efficient meshless method for fracture analysis of cracks", *Comput. Mech.*, **26**, 398-408.

Rice, J.R. (1968), "A path independent integral and the approximate analysis of strain concentration by notches and cracks", *J. Appl. Mech.*, **35**, 379-386.

Rice, J.R. and Tracey, D.M. (1973), *Computational fracture mechanics. Numerical and Computer Methods in Structural Mechanics*, Eds. Fenves, S.J. *et al.*, Academic Press.

Rooke, D.O. and Cartwright, D.J. (1976), *Compendium of Stress Intensity Factors*, The Hillingdon Press.

Shi, J., Ma, W. and Li, N. (2013), "Extended meshless method based on partition of unity for solving multiple crack problems", *Meccanica*, **43**(9), 2263-2270.

Singh, I.V., Mishra, B.K., Bhattacharya, S. and Patil, R.U. (2012), "The numerical simulation of fatigue crack growth using extended finite element method", *Int. J. Fatig.*, **36**, 109-119.

Strang, G. and Fix, G.J. (1973), *An Analysis of the Finite Element Method*, Prentice-Hall, New Jersey.

Sukumar, N., Moran, B. and Belytschko, T. (1998), "The natural element method in solid mechanics", *Int. J. Numer. Meth. Eng.*, **43**, 839-887.

Tong, P., Pian, T.H.H. and Lasry, S.J. (1973), "A hybrid element approach to crack problems in plane elasticity", *Int. J. Numer. Meth. Eng.*, **7**, 297-308.

Xiao, Q.Z., B.L. Karihaloo, B.L. and Liu, X.Y. (2004), "Direct determination of SIF and higher order terms of mixed mode cracks by a hybrid crack element", *Int. J. Fract.*, **125**, 207-225.

Yau, J.F., Wang, S.S. and Corten, H.T. (1980), "A mixed-mode crack analysis of isotropic solids using conservation laws of elasticity", *J. Appl. Mech.*, **47**, 335-341.

Yvonnet, J., Ryckelynck, D., Lorong, P. and Chinesta, F. (2004), "A new extension of the natural element method for non-convex and discontinuous problems: the constrained natural element method (C-NEM)", *Int. J. Numer. Meth. Eng.*, **60**(8), 1451-1474.

Zhang, Z., Liew, K.M., Cheng, Y. and Lee, Y.Y. (2008), "Analyzing 2D fracture problems with the improved element-free Galerkin method", *Eng. Anal. Bound. Elem.*, **32**, 241-250.

CC